2019 International Conference on Robotics and Automation (ICRA)
Palais des congres de Montreal, Montreal, Canada, May 20-24, 2019

Nitinol living hinges for millimeter-sized robots and medical devices

Peter A. York, *Student Member, IEEE* and Robert J. Wood, *Fellow, IEEE*

***Abstract*— A hybrid manufacturing process combining abrasive jet and laser micromachining enables the creation of living hinges in nitinol that retain the superelastic properties of the bulk material. The former selectively etches through the thickness of a workpiece and the latter defines the part's final geometry. Because the majority of the material removal is done with the room-temperature mechanical etching procedure, thermal damage to the part is minimized. Processing param-eters to achieve desired geometries are described, a bending stiffness model for the living hinges is provided, and validation experiments are presented. Lastly, to demonstrate the usefulness of these components to millimeter-sized robotic systems and medical devices, we show their integration in two prototype devices: an endoscopic camera wrist and a simple laser beam steering system.**

I. Introduction

Nitinol has numerous properties that recommend it as a material for biomedical applications, including its superelasticity, biocompatibility, kink resistance, torquability, and fatigue resistance in strain-controlled environments. By exploiting these properties, passive devices such as stents, catheter tubes, guide wires, and stone baskets enable less invasive interventions and better surgical outcomes than would be possible with more rigid stainless steel tools [1], [2]. Incorporating nitinol in active robotic devices is an ongoing research interest, marked by the development of a variety of robotic systems [3], [4], [5] and mechanisms [6], [7] that leverage nitinol's unique properties to facilitate minimally invasive surgical interventions. Core to these efforts have been the development of new fabrication and processing techniques for machining the material while retaining its superelastic structure. This work represents one such advance.

Indeed, the challenges of machining nitinol are well known: work hardening causes wear on mechanical cutting tools, laser processing results in a heat-affected zone (HAZ) and induces microcracks that must be removed in post processing, and wire electro-discharge machining (EDM) similarly induces microcracks and can leave a recast layer from the oxidation of the electrode. Additional challenges arise for machining operations more complex than simple through cutting. Pocketing – the creation of blind cavities – is one such operation. Thin, fragile mechanical cutting tools cannot be easily plunged into the workpiece, sink EDM requires the creation of a specialized electrodes [9], [10], and laser rastering to selectively remove material creates a large HAZ that leads to the embrittlement of the workpiece and the loss of superelasticity.

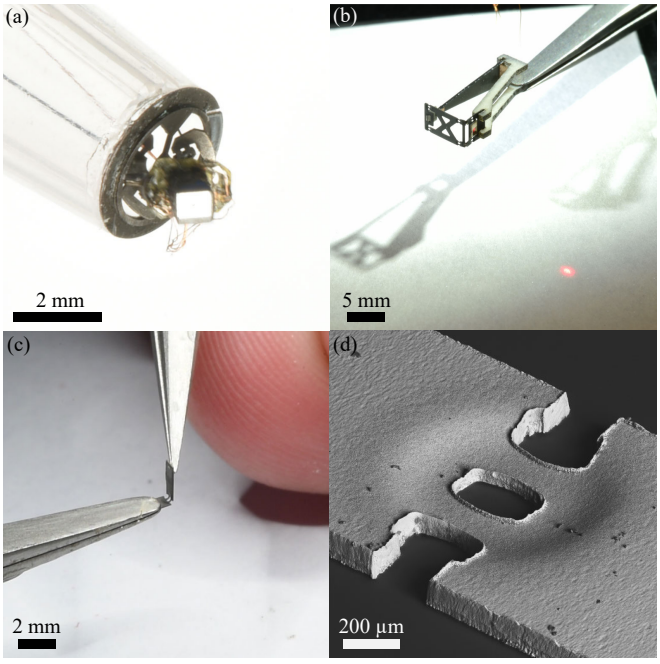

Fig. 1: (a) Spherical five-bar linkage fabricated with nitinol living hinges, used as a camera-steering mechanism actuated by pull wires. (b) Four-bar nitinol linkage driven by a piezoelectric actuator, orienting a mirror to steer a laser beam. (c) 10 µm nitinol hinge bent to 90°, showing the large elastic range of these components. (d) Scanning electron microscope image of a typical nitinol hinge, showing the reduction in thickness accomplished through mechanical etching.

Nevertheless, the ability to form blind cavities in nitinol is attractive because it would enable the creation of superelastic living hinges. Living hinges have well-defined rigid and flexible regions and are made from a single material. Superelastic hinges are of particular interest because of their large elastic limit (6-8%, typically, compared to 3% for polyimide, a commonly used flexure material). In general, living hinges facilitate the fabrication of complex mechanical systems while minimizing the number of parts needed, which simplifies assembly and joining processes. The latter benefit is potentially very relevant for nitinol, which is challenging to join to dissimilar metals and requires the use of interlayers [8]. Furthermore, living hinges allow devices to be made more compactly (especially in the thickness dimension), which is advantageous for microrobotic and biomedical devices, in which space and weight are at a premium [11], [12], [13]. Living hinges are a specific type of flexure, a compliant

This work was conducted using equipment supported by an ARO DURIP program (award #W911NF-13-1-0311). It was also funded in part by the Wyss Institute.

Peter York and Robert J. Wood are with the John A. Paulson School of Engineering and Applied Sciences, Harvard University, Cambridge, MA USA, pyork@g.harvard.edu, rjwood@eecs.harvard.edu

978-1-5386-6026-3/19/$31.00 ©2019 IEEE

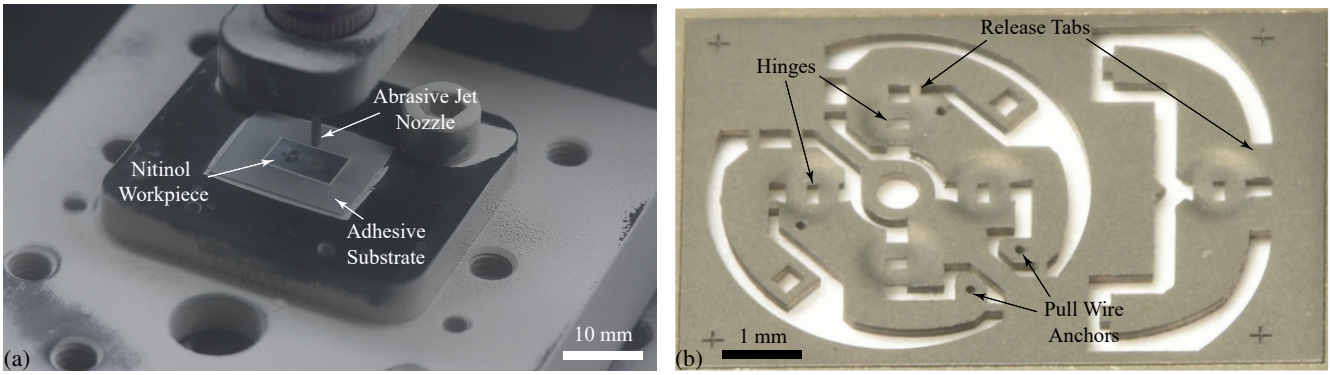

Fig. 2: (a): Abrasive jet micromachining setup. The nitinol workpiece is held by an adhesive substrate and positioned beneath the nozzle using an x-y stage (not shown). (b): Example parts fabricated with nitinol hinges. The thin hinge regions are formed through abrasive jet machining and the outline of the structure is defined via laser micromachining.

member that approximates the motion of a revolute joint. Within the context of millimeter-sized robots and medical devices, the primary appeal of compliant mechanisms based on flexures is that they allow the transmission of force and motion without bearing structures, which become inefficient, inaccurate, and challenging to fabricate as system size decreases.

The new fabrication approach described herein overcomes the manufacturing limitations posed by existing techniques by combining the meritorious features of two different methods: abrasive jet micromachining (AJM) and laser micromachining. Drawing inspiration from millimeter-scale fabrication of piezoceramics [14], we turned to AJM because it allows selective material removal through the thickness of a workpiece without a HAZ. In AJM, a fine powder consisting of hard particles is mixed with air and propelled in a fine jet to mechanically etch a solid surface. Blasting media size and type, pressure, nozzle distance, and other parameters can be tuned to achieve desired surface properties and etch rates [15]. Both masked and direct write methods can be used; we use a maskless method here because of the low etch rates of nitinol. With the maskless approach we use a horizontal x-y stage to control the nozzle location relative to the workpiece. After using AJM to modify a workpiece's thickness, we then use laser micromachining, which can make precise, high aspect ratio through-cuts, to define a part's final geometry in the lateral directions. Lastly, a low pressure AJM etch can be used to partially remove the HAZ generated by the laser (as employed during stent processing).

This new fabrication approach allows for the fabrication of living hinges in nitinol that retain the superelasticity of the bulk material. A simple prototype device to demonstrate the use of this method is shown in Fig. 1a; it consists of a single sheet of nitinol with rigid and flexible regions, with a single sheet of stainless steel bonded to the rigid regions to increase stiffness in those areas. The device, a spherical five-bar linkage, is shown controlling the orientation of a CMOS camera. We expect that distal dexterity mechanisms, thematically similar but more sophisticated than this simple demonstration, are a promising initial application area for this technology.

In this paper, we fully describe the living hinge manufacturing process, including key relationships between processing parameters and etch rates. We show the selectivity of the fabrication method through the fabrication of hinges of a range of thicknesses. To allow hinges to be properly sized for particular applications, we provide a model for bending stiffness that accurately captures their full superelastic behavior. We then validate the model through a series of experiments, describe initial fatigue tests, and discuss avenues for further development. We anticipate the broad usefulness of this technique to enable new capabilities in millimeter-size robots and medical devices.

II. Manufacturing

The flexures are fabricated from a superelastic nitinol sheet (Johnson Matthey PLC). Square centimeter samples are mounted on a strong two-sided adhesive (Gel-Pak x8, Delphon Industries) and mounted on an x-y stage inside an AJM station (ProCenter Plus, Comco Inc). See Fig. 2a. A controllable vertical stage rigidly holds the nozzle and controls its distance to the sample. Because we used a direct write method, the x-y stages are necessary to position the sample relative to the nozzle. This allows flexures to be precisely placed on a single sheet, which can then be incorporated as a flexible layer in a multi-material laminate or directly used in a device. Samples can also be post-processed using other micromachining tools, such as tabletop mills, wire EDM, or laser cutters to make through-cuts and define the margins of the flexible regions. For example, to define the geometry shown in Fig. 2b, we used an Nd:YAG laser (Coherent Avia 355-7) integrated in a laser micromachining center (Oxford Lasers, E Series). The center is removed from each flexure because it was seen that slightly more material remained at the center of the etch areas than the edges, likely due to the particle ejection dynamics.

In order to create flexures of predictable thickness, we characterized the vertical and lateral etch rates for two key processing parameters that are easily varied: pressure and nozzle distance (Fig. 3). Both vertical and lateral etch

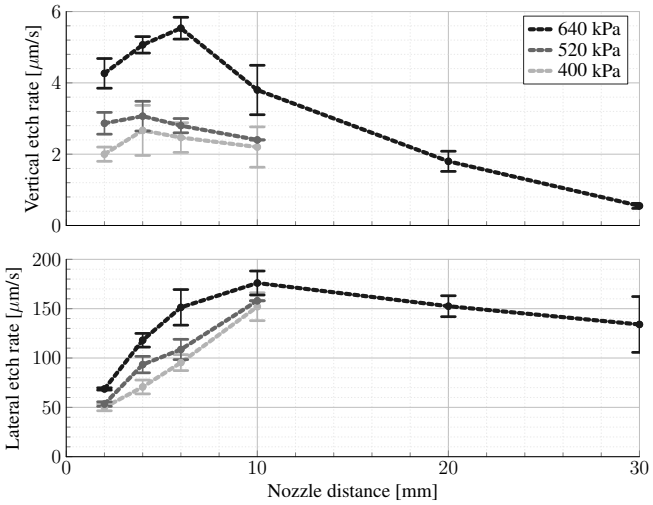

Fig. 3: Vertical and lateral etch rates for nitinol at various pressures and standoff distances. The same blasting media (10 μm alumina) and nozzle diameter (450 μm) were used for all tests.

rates initially increase with increasing nozzle distance before falling rapidly off. The vertical etch rate is very sensitive to pressure while the lateral etch rate is largely agnostic to it. For all tests we held nozzle diameter (450 μm) and blasting media type (10 μm alumina) constant. Those parameters were chosen with a view toward minimizing feature size. The etch profiles were measured on a confocal microscope (Olympus LEXT OLS4000), and then the etch rates were calculated based on the time of each etch.

III. MODELING

With a view towards designing flexures for particular applications, we devised a model for predicting bending stiffness as a function of geometry; geometric parameters are shown in Fig. 4. Bending stiffness is nonlinear with flexure angle due to nitinol's superelasticity, which can be described in the simplified "bilinear" model:

$$\sigma(\epsilon) = \begin{cases} -E\epsilon_\ell + E_n(\epsilon + \epsilon_\ell) & \epsilon < -\epsilon_\ell \\ E\epsilon & -\epsilon_\ell \leq \epsilon \leq \epsilon_\ell \\ E\epsilon_\ell + E_n(\epsilon - \epsilon_\ell) & \epsilon > \epsilon_\ell \end{cases} \quad (1)$$

Where $\epsilon_\ell = \sigma_{cr}/E$ is the elastic limit of the austenitic phase, σ_{cr} is the stress just before stress-induced martensite begins to form (nucleation), and E is the elastic modulus of the austenitic phase. The elastic modulus of the mixed austenitic/martensitic phase, E_n, is much lower than E.

We assume that the assumptions of constant curvature bending apply and note that it will begin to fail as the ratio t/ℓ increases. Under those assumptions, pure bending about the x-axis will result in strain linearly distributed about the bending plane, and given by:

$$\epsilon(y, \theta) = \frac{y\theta}{\ell} \quad (2)$$

The moment-angle relationship can be calculated first by

Material Properties		Geometric Parameters	
E	50 GPa	w	400 μm
E_n	7 GPa	ℓ	200 μm
σ_{cr}	750 MPa	t	15 to 50 μm
ϵ_ℓ	1.5 %		

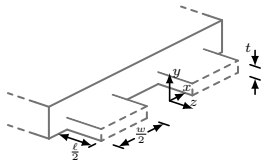

Fig. 4: Material properties and geometric parameters for the fabricated flexure hinges, with a schematic representation for reference.

defining the strain energy density at a single strain state as:

$$W(\epsilon) = \int_0^\epsilon \sigma(e)\, de \quad (3)$$

Then, by integrating the strain energy density with respect to the flexure volume, the total strain energy density can be calculated.

$$U(\theta) = \int_V W(\epsilon(y, \theta))\, d\mathcal{V} \quad (4)$$

Lastly, Castigliano's first theorem can be directly applied to compute the moment generated by the hinge for a given angle of rotation:

$$M = \frac{\partial U(\theta)}{\partial \theta} \quad (5)$$

IV. CHARACTERIZATION

To validate our model and demonstrate the versatility of the manufacturing process for producing flexures with particular stiffness, we fabricated flexures of varying thicknesses and characterized them using the test setup shown in Fig. 5a. A flexure is held vertically between two rigid pieces of a thick fiber reinforced composite (FR4, 450 μm). One side of the flexure is rigidly attached to a servo and the other side is allowed to slide against an arm that is rigidly attached to a high-resolution six-axis force/torque sensor (ATI Nano-17 Titanium, SI-8-0.05, ATI Industrial Automation). The bending moment generated by the flexure is measured about the z-axis of the sensor, which has suitable resolution (<1 N μm after filtering) for resolving the generated moments, which range from 20 to 200 N μm.

For each test, the servo was driven with a cyclic motion profile with frequency ∼1 Hz and magnitude appropriate to not plastically deform the flexure under test. Data was collected from the force/torque sensor at 1 kHz, processed with a 100-order median filter (chosen to reduce signal noise while preserving the signal edges), and averaged over the loading cycles. Five cycles were used for each flexure, which was sufficient to reduce the standard deviation for each measurement to within 10 % of its mean value. We assumed that the servo followed a constant velocity profile except for short ramping periods at the extreme points of its trajectory. The flexure angle was then calculated from the servo angle as a function of the link lengths of the test setup.

The results, presented in Fig. 5b, demonstrate our model's ability to predict both the absolute stiffness of different sized flexures as well as the nonlinear loading path that each takes. The initial loading regions correspond to the predominance of austenite and the plateau regions that follow correspond

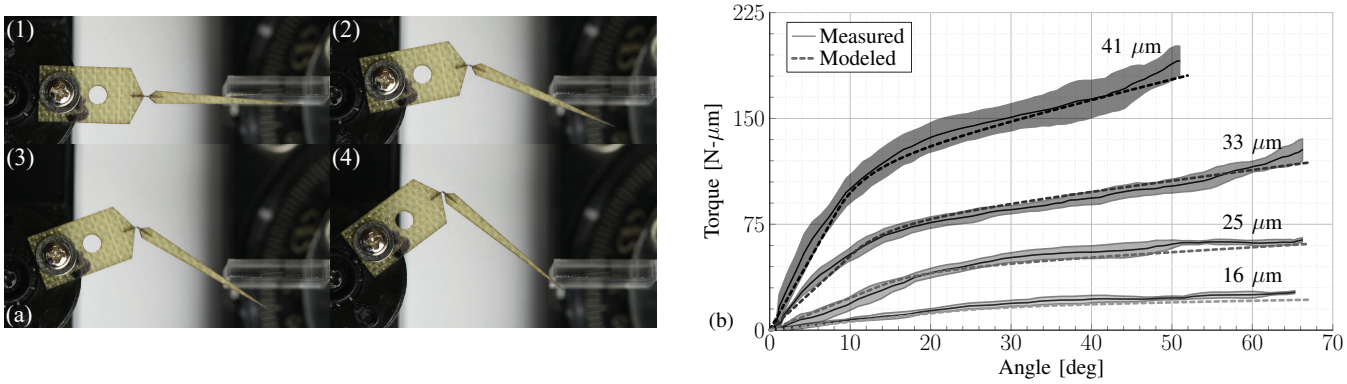

Fig. 5: (a): Experimental setup for measuring the torque profiles of the flexure hinges. The servo (at left) controlled the angle of the flexure hinge (center) relative to the force/torque sensor (out of page, right). All tests were conducted quasi-statically at a loading frequency of $\sim$1 Hz. The sequence shows elastic deformation of the flexure under test from 0 to 70°. (b): Experimentally measured and modeled torque vs. angle profiles for a range of hinge thicknesses. Experimental data was gathered under displacement control and averaged over five cycles. The mean and standard deviation of the measured data are shown for each flexure. The model captures the flexures' nonlinear behavior and reasonably predicts their torque vs. angle profiles.

to the nucleation of stress-induced martensite. The critical torque that marks the transition between the two regimes for each flexure is seen to be roughly quadratic with thickness, as expected from classic beam theory.

V. Prototype Devices

The first prototype device, shown in Fig. 1a, incorporates four living hinges in a spherical five-bar mechanism. Its constituent parts are shown in Fig. 2b: a flat piece with the four hinges arranged radially symmetric about the device center and a second piece that connects across the top of the device to constrain the linkage to spherical motion. Release tabs are used to limit off-axis forces on the flexures during assembly. The linkage is actuated by four pull wires that anchor to the structure through micro holes drilled using laser micromachining. Each wire corresponds to bending in one quarter of the hemispherical workspace of the spherical five bar. Because of the small size of the device, the effective moment arms between the pull wire anchors and the flexures are quite short, and thus the amount of shearing in the flexures and the force required to generate bending is significant. To ameliorate this effect to some degreee, we added a stainless steel backing to enhance the stiffness of the rigid regions of the nitinol workpiece and thus better define the joint centers.

In the second prototype device, shown in Fig. 1b and Fig. 6, a laser beam is steered using a mirror attached to the pivot link of a four-bar mechanism formed from contiguous nitinol with well-defined hinge and structural regions. The linkage was made from two separate nitinol pieces, joined together via laser welding. The slider of the mechanism is driven by a piezoelectric bending actuator. This device well-illustrates the value of the living hinge approach: a minimum of components and materials are need to achieve the motion transmission from the quasi-linear motion of the piezoceramic to the rotational motion of the mirror.

VI. Discussion

Though the direct write etching method described herein allows for the fabrication of simple hinges, it cannot produce the complex geometries that would be possible with a masked process. We conducted initial experiments in this direction using a commercially available dry film photoresist specifically formulated for sandcarving (4 mil RapidMask High Tack, Ikonics Corp), but we were unable to find suitable processing parameters that resulted in faster etching through nitinol than the resist. We expect that a suitable

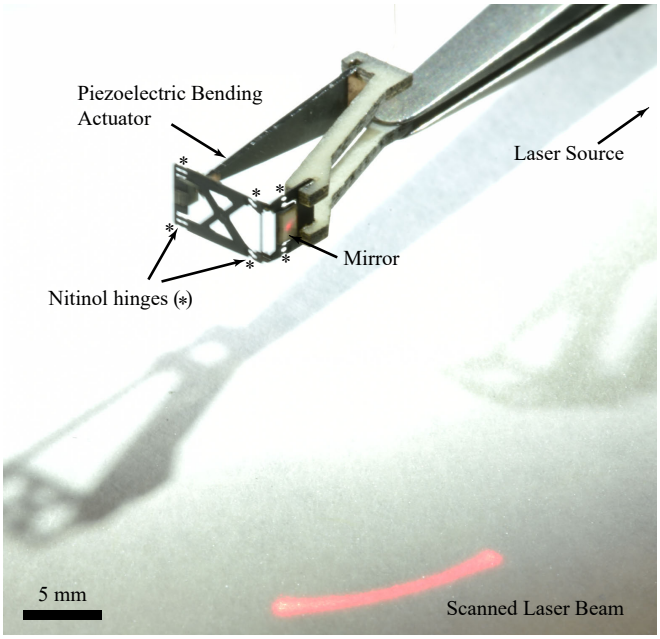

Fig. 6: Laser scanning device fabricated using the procedure described in this work. A piezoelectric bending actuator provides a linear input to a four-bar linkage consisting of rigid and flexible regions of nitinol. A mirror on the pivot link of the linkage steers the laser beam along an arc as shown. The image was captured with a long exposure to show the range of motion of the linkage.

mask will be hard to find because of the relatively slow etch rate of nitinol. This can be seen by comparing it to a material more suitable for abrasive jet etching, such as glass or the piezoceramic described in [14]. The reported etch rates for the piezoceramic were $\sim$50x higher for similar processing conditions and required standoff distances on the order of centimeters instead of millimeters. Though masking seems like an implausible path for to achieve greater etch complexity, CNC tooling seems like a natural next step in the development of this technique. The abrasive jet stream could be continuously moved relative to the workpiece in order to create complex 2.5D etch patterns.

We conducted initial experiments into the living hinges' fatigue life and found that they failed at around 2000 cycles when cycled at $1\,\mathrm{Hz}$ from unloaded to $6\,\%$ strain. Nitinol fatigue life is governed by crack initiation rather than crack propagation [16], and thus preventing or limiting microcrack formation during fabrication is a primary concern. Fatigue properties can be improved by electropolishing and thermal treatment [17], and thus we expect an exploration of the techniques to be a natural extension of the work described herein.

VII. CONCLUSION

A new method was proposed for fabricating living hinges out of nitinol, such that the superelasticity of the bulk material is retained after fabrication. Two prototype devices were presented that demonstrate the motion transmission capabilities enabled by this process. Using the model and processing parameters described, these hinges can be properly sized for given loading and displacement conditions, and we anticipate that they will be broadly useful in a variety of millimeter-sized robotic and medical device contexts, in which large ranges of motion are needed in compact spaces.

VIII. ACKNOWLEDGMENTS

The authors thank James Weaver for his acquisition of the SEM image and Elizabeth Helbling for her timely assistance.

REFERENCES

[1] T. Duerig, A. Pelton, and D. Stöckel, "An overview of nitinol medical applications," *Materials Science and Engineering: A*, vol. 273, pp. 149–160, 1999.

[2] D. Kapoor, "Nitinol for medical applications: A brief introduction to the properties and processing of nickel titanium shape memory alloys and their use in stents," *Johnson Matthey Technology Review*, vol. 61, no. 1, pp. 66–76, 2017.

[3] P. E. Dupont, J. Lock, B. Itkowitz, and E. Butler, "Design and control of concentric-tube robots," *IEEE Transactions on Robotics*, vol. 26, no. 2, pp. 209–225, 2010.

[4] N. Simaan, R. Taylor, and P. Flint, "A dexterous system for laryngeal surgery," *IEEE International Conference on Robotics and Automation*, vol. 1, pp. 351–357, 2004.

[5] R. J. Hendrick, S. D. Herrell, and R. J. Webster, "A multi-arm hand-held robotic system for transurethral laser prostate surgery," in *Robotics and Automation (ICRA), 2014 IEEE International Conference on*. IEEE, 2014, pp. 2850–2855.

[6] W. Sieklicki, M. Zoppi, and R. Molfino, "Superelastic compliant mechanisms for needlescopic surgical wrists," *ASME/IFToMM International Conference on Reconfigurable Mechanisms and Robots*, pp. 392–399, 2009.

[7] P. J. Swaney, P. A. York, H. B. Gilbert, J. Burgner-Kahrs, and R. J. Webster, "Design, fabrication, and testing of a needle-sized wrist for surgical instruments," *Journal of medical devices*, vol. 11, no. 1, p. 014501, 2017.

[8] M. H. Wu, "Fabrication of nitinol materials and components," in *Materials Science Forum*, vol. 394. Trans Tech Publ, 2002, pp. 285–292.

[9] J. Yan, T. Kaneko, K. Uchida, N. Yoshihara, and T. Kuriyagawa, "Fabricating microgrooves with varied cross-sections by electrodischarge machining," *The International Journal of Advanced Manufacturing Technology*, vol. 50, no. 9-12, pp. 991–1002, 2010.

[10] M. Hourmand, A. A. Sarhan, and M. Sayuti, "Micro-electrode fabrication processes for micro-edm drilling and milling: a state-of-the-art review," *The International Journal of Advanced Manufacturing Technology*, vol. 91, no. 1-4, pp. 1023–1056, 2017.

[11] K. Y. Ma, P. Chirarattananon, S. B. Fuller, and R. J. Wood, "Controlled flight of a biologically inspired, insect-scale robot," *Science*, vol. 340, no. 6132, pp. 603–607, 2013.

[12] N. Doshi, B. Goldberg, R. Sahai, N. Jafferis, D. Aukes, R. J. Wood, and J. A. Paulson, "Model driven design for flexure-based microrobots," in *Intelligent Robots and Systems (IROS), 2015 IEEE/RSJ International Conference on*. IEEE, 2015, pp. 4119–4126.

[13] Y. Zou, W. Zhang, and Z. Zhang, "Liftoff of an electromagnetically driven insect-inspired flapping-wing robot," *IEEE Transactions on Robotics*, vol. 32, no. 5, pp. 1285–1289, 2016.

[14] I. Misri, P. Hareesh, S. Yang, and D. DeVoe, "Microfabrication of bulk PZT transducers by dry film photolithography and micro powder blasting," *Journal of Micromechanics and Microengineering*, vol. 22, no. 8, p. 085017, 2012.

[15] A. Ghobeity, H. Getu, T. Krajac, J. Spelt, and M. Papini, "Process repeatability in abrasive jet micro-machining," *Journal of materials processing technology*, vol. 190, no. 1-3, pp. 51–60, 2007.

[16] M. Mahtabi, N. Shamsaei, and M. Mitchell, "Fatigue of nitinol: the state-of-the-art and ongoing challenges," *journal of the mechanical behavior of biomedical materials*, vol. 50, pp. 228–254, 2015.

[17] G. Condorelli, A. Bonaccorso, E. Smecca, E. Schäfer, G. Cantatore, and T. Tripi, "Improvement of the fatigue resistance of niti endodontic files by surface and bulk modifications," *International endodontic journal*, vol. 43, no. 10, pp. 866–873, 2010.